ACS OMEGA

http://pubs.acs.org/journal/acsodf

Article

Geochemical Signatures and Controlling Factors of Rearranged Hopanes in Source Rocks and Oils from Representative Basins of China

Yao-Ping Wang,* Xin Zhan, Yuan Gao, Jia Xia, Sibo Wang, and Yan-Rong Zou

Cite This: *ACS Omega* 2020, 5, 30160−30167

Read Online

ACCESS | Metrics & More | Article Recommendations

ABSTRACT: The origin and geochemical significance of the rearranged hopanes in hydrocarbon source rocks or crude oil have attracted extensive attention. Despite numerous studies, there is not yet a proper conclusion. Therefore, this paper discusses the formation conditions of such compounds and points out their geochemical significance in more detail using a remarkably broad range of source rocks and crude oils from four basins in China. Varying content of rearranged hopanes was found in a total of 19 source rocks and oils from the Ordos, Sichuan, and Tarim basins and the North China Block. Gas chromatography−mass spectrometry (GC−MS) in combination with X-ray diffraction (XRD) and conventional geochemical parameters was used for Pearson correlation analysis to reveal the enrichment mechanisms of rearranged hopanes in the studied rock and oil samples. The GC−MS and XRD results showed that the studied source rocks with high rearranged hopane contents are closely associated with the high abundance of quartz rather than that of clay. Furthermore, the present study reveals that anoxic lacustrine conditions are the primary controlling factors of relatively high abundance of rearranged hopanes in the studied rocks and oils, whereas thermal maturity and terrigenous organic matter input are the secondary factors.

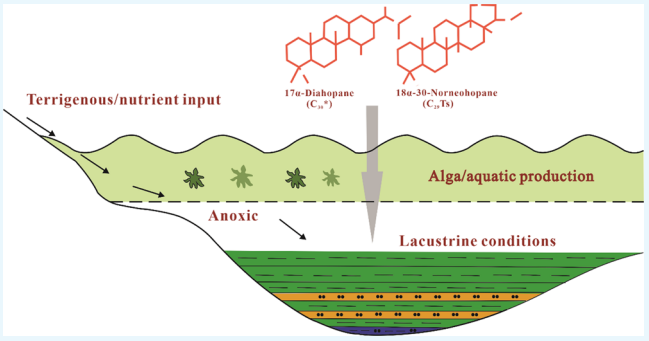

1. INTRODUCTION

Rearranged hopanes are compounds with the same carbon framework as that of normal hopanes, whereas the position of the methyl side chain in rearranged hopanes differs from that in normal hopanes.[1] A series of homologues has been identified in source rocks and oils, predominantly including 18α(H)-hopane series (C_{27} trinorhopane (Ts) and C_{29} norhopane (C_{29}Ts)), 17α(H)-diahopane series (C_{29}−C_{35} rearranged hopanes, with the C_{30} rearranged hopane as the main peak), 21-methyl-28-norhopane series, and C_{30} early-eluting rearranged hopane series (C_{30}E).[2−5]

Possible biological sources and formation environments of these rearranged hopanes have been widely discussed after their identification. Previous studies suggested that abundant rearranged hopanes are formed with sources of terrigenous organic matter, especially bacterially reworked higher plants[6−8] or benthic red macroalgae[9,10] and clay-induced mediator acidic catalysis under oxic and suboxic conditions,[11−13] a brackish-to-freshwater environment or diagenesis,[6,8,14] clay-catalyzed reactions in suboxic conditions,[15] a suboxic brackish water environment,[16−18] and an anoxic and brackish-saline environment.[19] Thus, rearranged hopanes were used to interpret source inputs of bacterially reworked higher plants and/or depositional conditions of acidic clay catalysis in oxic−suboxic environments.

Surprisingly, few studies systematically reviewed the literature on the influence of the depositional environment on rearranged hopanes in rocks and oils in representative basins, although many source rocks and oils with the high abundance of rearranged hopanes were identified especially in the Ordos Basin,[15,17,20,21] Sichuan Basin,[14,22] North China Block,[10,23] and Tarim Basin.[12,17] Thus, this study set out to systematically investigate the influence of critical environmental factors on the occurrence of rearranged hopanes through a comparative study of source rocks and oils from the Ordos, Sichuan, and Tarim basins and the North China Block.

Received: September 19, 2020
Accepted: November 2, 2020
Published: November 12, 2020

https://dx.doi.org/10.1021/acsomega.0c04615
ACS Omega 2020, 5, 30160−30167

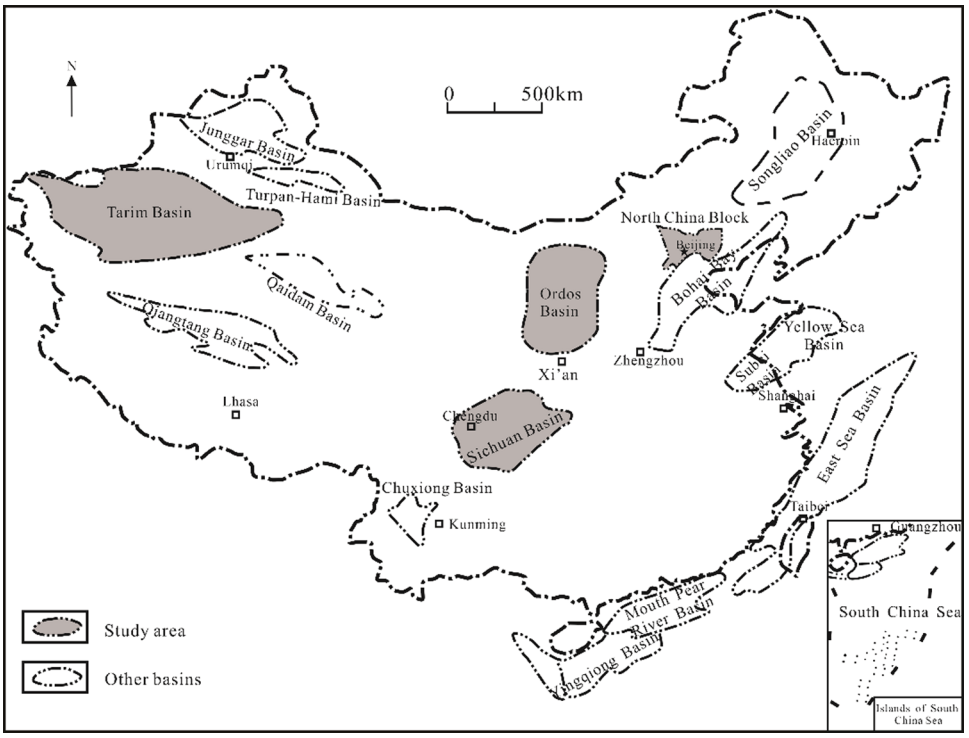

Figure 1. Map showing the location of the Ordos, Sichuan, and Tarim basins and the North China Block.[23,24]

2. GEOLOGICAL BACKGROUND

Rearranged hopanes are rich in source rocks or crude oils from the Ordos, Sichuan, and Tarim basins and the North China Block. Figure1 displays the location of the study area within China.

2.1. The Ordos Basin. The source rocks used in this paper were partially selected from the Tongchuan area in the southern Ordos Basin, which is the second largest sedimentary basin in western China, covering up to ∼250,000 km^2 of area.[17] The Ordos Basin is bounded to the north by the Yinshan Mountains, to the south by the Qinling Mountains, to the west by the Liupanshan Mountains, and to the east by the Luliangshan east.[15] This basin consists of six structural units: the Yimeng Uplift, Weibei Uplift, Tianhuan Depression, Shanbei Slope, Jinxi Flexural Fold Belt, and Western Edge Thrusting Belt.[15] It is predominantly filled with Paleozoic, Mesozoic, and Cenozoic sediments with giant oil reservoirs concentrated in the Mesozoic fluvial−lacustrine deposits.[25] The vast majority of the oil resources (∼75%) among Mesozoic petroleum systems are discovered in the Upper Triassic Yanchang Formation.[26] The Yanchang Formation consists of 10 bottom-up members (Chang 10 to Chang 1) based on the lithology and sequence stratigraphy.[26] Particularly, sandstones in Chang 8 and 6 members are the primary oil reservoirs, whereas shales and siltstones in Chang 7 are recognized as the best source rock member for the Ordos Basin.[27]

2.2. The Sichuan Basin. The source rocks used in this paper were partially selected from the Upper Permian Longtan Formation in the Eastern Sichuan Basin. It is a superimposed basin located in southwest China and undergoes multiple sedimentary cycles, covering up to ∼230,000 km^2 of area.[22] The Sichuan Basin consists of four basic structural units: the eastern depression, western depression, central uplift, and southern depression.[28] It experienced two major tectonic movements, including early-phase passive continental margin tectonics from the Paleozoic to the Early Triassic and the late-phase foreland basin stage from the Late Triassic to the Eocene.[22,29] Six hydrocarbon-rich strata, including Cambrian, Silurian, Carboniferous, Permian, Triassic, and Jurassic, have been found in the Sichuan Basin.[30] Three major series of marine source rocks among the six strata are distributed in the Cambrian strata ($\in_1$j, $\in_1$n, and $\in_1$q), Longmaxi Formation (S_1l), and Longtan Formation (P_2l).[31]

2.3. The North China Block. The source rocks used in this paper were partially selected from Unit 3 of the Xiamaling Formation in the North China Block. This formation is predominantly distributed within the Yanliao Depression of the North China Block in latitudes of 10−30°N.[32] Recent zircon U−Pb dating of K-bentonite beds in this formation yields an age of 1368 ± 12 Ma,[33,34] showing that it is formed during the Mesoproterozoic Era. It consists of six units (Unit 6 to Unit 1) from bottom to top, in total with a thickness of ∼450 m.[23] Unit 6 is mainly composed of cross-bedded sandstones and siltstones. Unit 5 is characterized by brown marlstones interbedded with laminated shales, organic-poor siltstones, and sandstones. Unit 4 consists mainly of alternating red and green mudstones and green sandy siltstones. The lithology of Unit 3 varies from bottom to top, with green siltstones at the bottom followed by interbedded black shales and chert in the middle, and black shales at the top. Unit 2 is characterized by thick black shales, and Unit 1 contains interbedded black and green shales.[35,36]

2.4. The Tarim Basin. The crude oils used in this paper were partially selected from the southwest depression in the Tarim Basin, which is located in northwestern China and one of the most petroliferous basins in this country, covering up to ∼560,000 km^2 of area.[37] This basin includes six first-order tectonic units, including the southwest depression, Kuqa Depression, Tazhong Uplift, Tabei Uplift, north depression,

https://dx.doi.org/10.1021/acsomega.0c04615
ACS Omega 2020, 5, 30160−30167

Table 1. Rock-Eval Data of the Source Rock Samples from the Ordos and Sichuan basins and the North China Block

basin	formation	lithology	depth (m)	sample	TOC	S_1	S_2	PI	T_{max}	S_3	HI	OI
Ordos Basin	Yanchang Formation/ Chang 7	oil shale	outcrop	TNH-1.5	13.08	2.43	53.48	0.04	436	0.66	409	5
	Yanchang Formation/ Chang 7	oil shale	outcrop	TNH-3.4	16.07	3.58	74.91	0.05	433	1.01	466	6
North China Block	Xiamaling Formation/Unit 3	oil shale	/	gxhy	5.32	0.62	18.74	0.03	433	2.20	352	41
	Xiamaling Formation/Unit 3	oil shale	/	dxhy	0.86	0.485	1.825	0.21	429	0.64	214	75.5
Sichuan Basin	Longtan Formation	black shale	328	10-VI-9	1.88	0.20	0.70	0.23	473	1.22	37	66
	Longtan Formation	black shale	334.7	10-VI-31	1.32	0.12	0.31	0.27	461	0.53	23	40
	Longtan Formation	black shale	414.6	10-VI-50	2.97	0.12	0.72	0.15	483	0.55	24	19
	Longtan Formation	black shale	457	10-VI-56	4.22	0.23	1.70	0.12	482	0.59	40	14

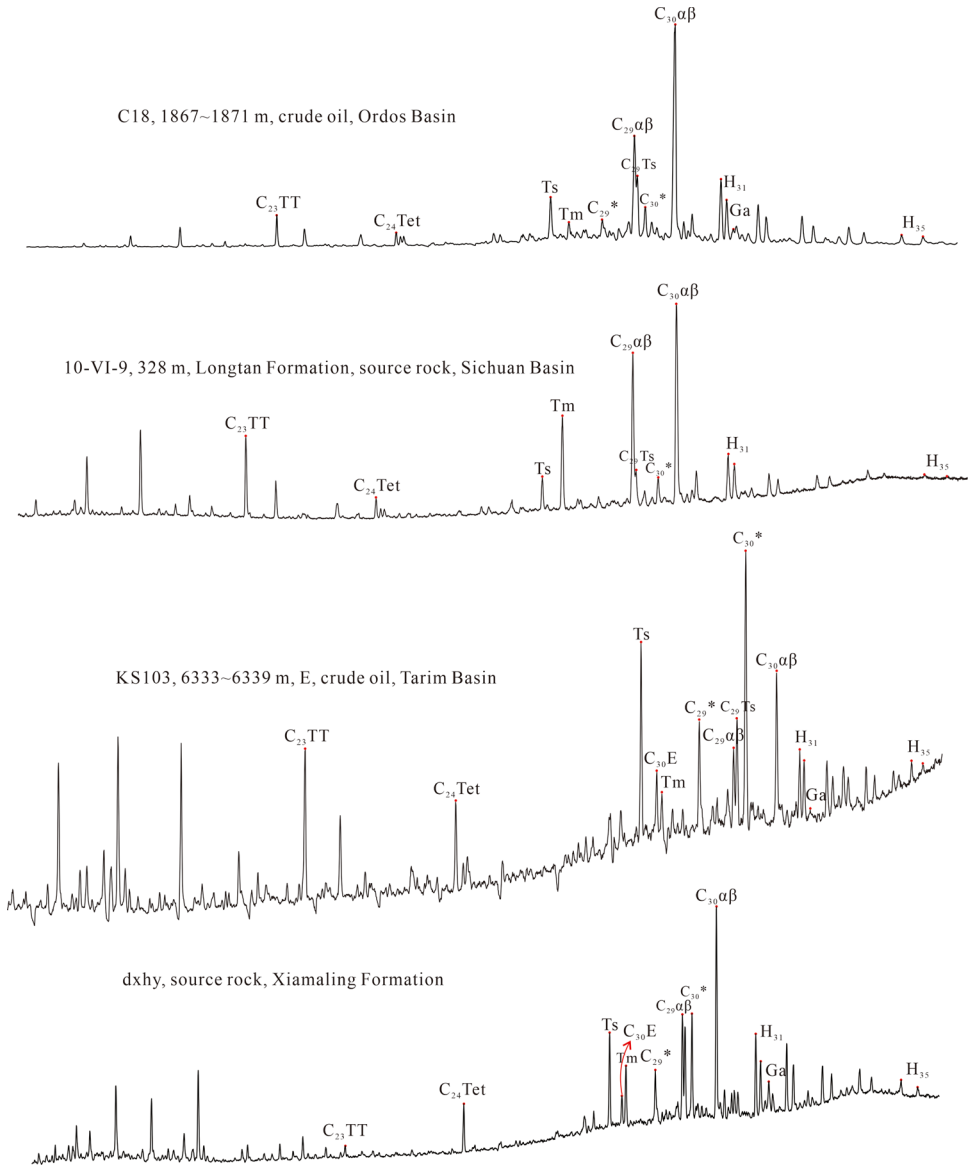

Figure 2. Mass spectrum (m/z 191) of the representative samples from the Ordos, Sichuan, and Tarim basins and the North China Block.

and southeast faulted-uplift zone.[38,39] The southwest depression currently has three major oil−gas fields, including the Kekeya oil field, Kedong gas field, and Akemomu gas field, with strata of promising hydrocarbon reservoirs concentrated in Neogene, Paleogene, Cretaceous, Carboniferous, Silurian, and Ordovician.[40] The two main series of source rocks are marine carbonate rocks and mudstones in the Carboniferous-Lower Permian and lacustrine-swamp coal-bearing sandy mudstones in the Lower-Middle Jurassic.[12,41]

3. SAMPLES AND ANALYTICAL METHODS

3.1. Samples. In total, 19 source rock and oil samples were used in this paper. Two oil shales and two crude oils were

https://dx.doi.org/10.1021/acsomega.0c04615
ACS Omega 2020, 5, 30160−30167

Table 2. Mineral Composition of the Source Rocks from the Ordos and Sichuan Basins and the North China Block

basin	sample	quartz	feldspar	illite	chlorite	kaolinite	calcite	dolomite	high-Mg calcite	siderite	pyrite
Sichuan Basin	10-VI-9	14.7	9.6	10.1	15	0	15.2	8.3	15.3	11.8	0
	10-VI-31	15	0	50.1	18.6	0	16.4	0	0	0	0
	10-VI-50	6.6	0	47.5	0	42.8	0	0	0	0	3.1
	10-VI-56	9.5	0	41.2	0	34.2	0	3.3	0	9.4	2.4
North China Block	dxhy	81.1	0	18.9	0	0	0	0	0	0	0
	gxhy	53.4	0	40.9	0	5.7	0	0	0	0	0
Ordos Basin	TNH1.5	19.5	21.6	37.8	15.6	0	0	0	0	0	5.6
	TNH3.4	24.9	22	42.9	0	0	0	0	0	0	10.3

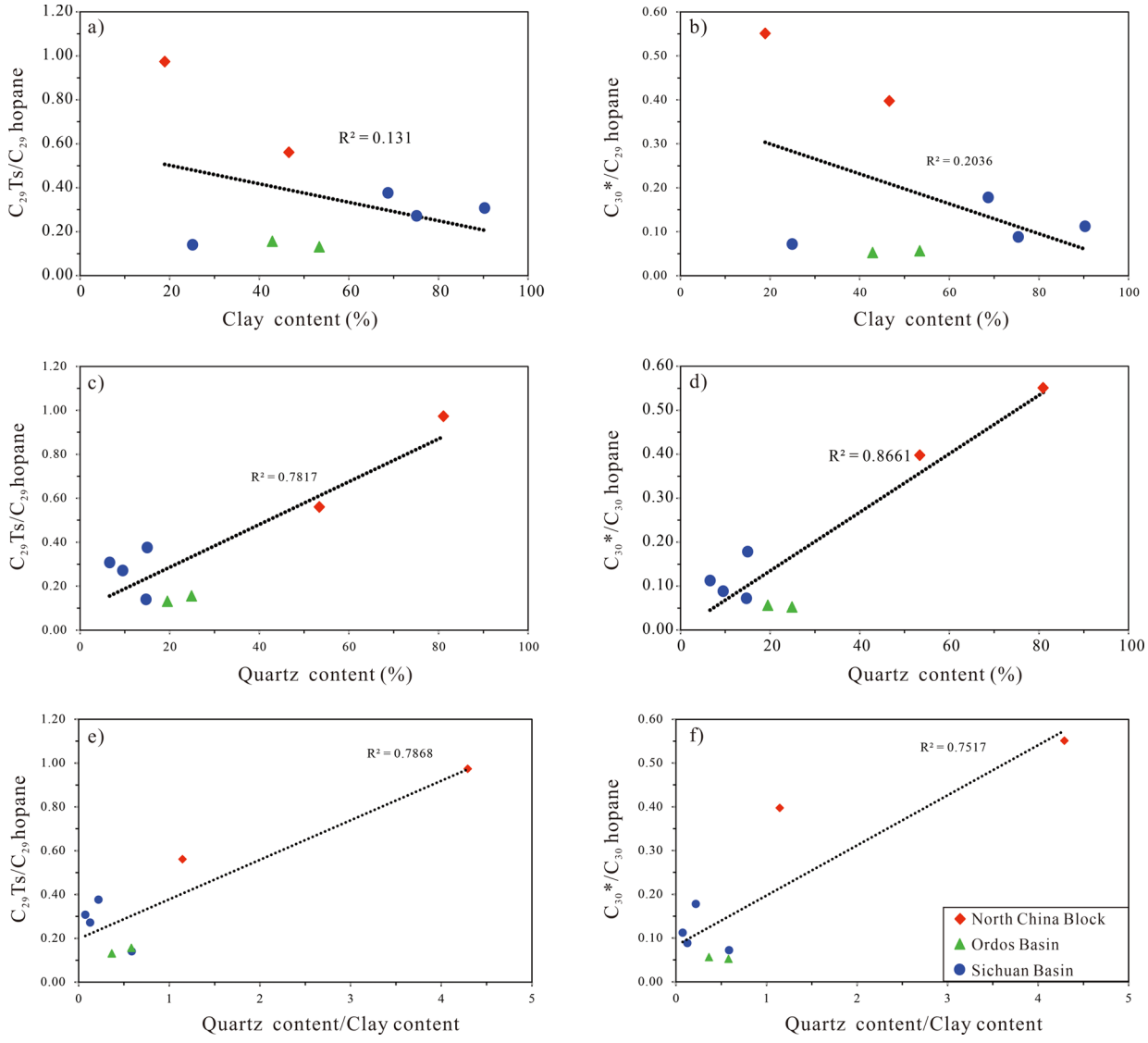

Figure 3. Cross plots of the content of rearranged hopanes and selected minerals, showing the possible connection between the rearranged hopanes and the quartz instead of clay minerals. (a) Clay content (%) versus $C_{29}Ts/C_{29}$ hopane; (b) clay content (%) versus $C_{30}*/C_{29}$ hopane; (c) quartz content (%) versus $C_{29}Ts/C_{29}$ hopane; (d) quartz content (%) versus $C_{30}*/C_{29}$ hopane; (e) quartz content/clay content versus $C_{29}Ts/C_{29}$ hopane; and (f) quartz content/clay content versus $C_{30}*/C_{29}$ hopane.

collected from the Ordos Basin, four black shales were gathered from eastern Sichuan Basin, two oil shales were collected from the Xiamaling Formation in the North China Block, and nine crude oils were selected from the southwest depression in the Tarim Basin.

3.2. Analytical Methods. All source rock samples were first ultrasonically cleaned using deionized water, then dried at 60 °C, and crushed into powder of 200 mesh. An IFP Rock-Eval 6 instrument was used to perform the pyrolysis analysis of the powdered samples. The powdered samples were initially heated to 300 °C in 3 mins to obtain the free hydrocarbon amount (S_1) and then heated from 300 to 650 °C with a rate of 25 °C per minute to measure the remaining hydrocarbon generative potential (S_2). Furthermore, dissolved organic matter was obtained from powdered samples using a Soxhlet apparatus with dichloromethane/methanol in 93:7 v/v for 72

https://dx.doi.org/10.1021/acsomega.0c04615
ACS Omega 2020, 5, 30160−30167

Table 3. Selected Biomarker Ratios of Source Rocks and Crude Oils from the Ordos, Sichuan, and Tarim basins and the North China Block[a]

basin	formation/ member	lithology	sample	R1	R2	R3	R4	R5	R6	R7	R8	R9	R10	R11	R12
Ordos Basin	Yanchang/ Chang 7	oil shale	TNH3.4	0.74	0.14	0.58	0.12	0.26	1.17	0.16	0.05	0.32	25.24	28.79	45.98
	Yanchang/ Chang 7	oil shale	TNH1.5	0.67	0.19	0.66	0.13	0.19	1.27	0.13	0.06	0.33	29.42	17.21	53.36
Sichuan Basin	Longtan Formation/P_2l	black shale	10-VI-9	0.67	0.21	0.42	0.15	0.22	0.75	0.19	0.08	0.38	27.68	23.77	48.55
	Longtan Formation/P_2l	black shale	10-VI-31	0.64	0.30	0.65	0.16	0.21	0.61	0.38	0.18	0.48	33.62	25.24	41.15
	Longtan Formation/P_2l	black shale	10-VI-50	0.56	0.37	0.65	0.18	0.15	0.81	0.31	0.11	0.41	32.57	25.30	42.13
	Longtan Formation/P_2l	black shale	10-VI-56	0.85	0.28	0.66	0.16	0.21	0.67	0.27	0.09	0.43	31.36	24.36	44.28
North China Block	Xiamaling Formation /Unit 3	oil shale	gxhy	0.63	0.34	0.55	0.26	2.54	0.86	0.56	0.40	0.29	24.92	29.36	45.72
	Xiamaling Formation/ Unit 3	oil shale	dxhy	0.63	0.89	0.48	0.23	2.36	0.48	0.97	0.53	0.35	17.70	20.48	61.83
Ordos basin	/	crude oil	h31	0.57	2.82	0.46	0.13	0.24	1.69	0.67	0.26	0.53	19.80	34.14	46.06
	/	crude oil	C18	0.85	0.33	0.77	0.15	0.19	1.15	0.46	0.12	0.46	24.15	27.13	48.72
Tarim basin	/	crude oil	KS101	1.31	0.51	1.09	0.29	0.49	0.96	0.27	0.14	0.44	21.25	26.87	51.88
	N1	crude oil	K20	1.15	0.73	2.36	0.25	1.25	2.26	0.96	1.70	0.60	23.64	19.49	56.87
	N1	crude oil	K10	1.49	2.43	0.54	0.15	0.86	0.92	0.14	0.13	0.51	9.90	34.40	55.70
	N_1	crude oil	KS709	1.16	0.49	4.74	0.32	1.09	1.75	1.39	1.80	0.62	20.94	34.04	45.02
	K_2	crude oil	Kd1	1.19	0.45	0.97	0.28	0.93	0.82	1.27	0.94	0.59	11.93	32.41	55.66
	E	crude oil	KS103	1.12	0.86	1.41	0.41	0.73	1.21	1.56	1.98	0.56	13.23	33.53	53.24
	N_1	crude oil	K2	1.12	0.42	2.53	0.77	0.98	1.31	1.63	3.27	0.63	14.42	35.72	49.86
	/	crude oil	Q3C	1.75	2.80	0.61	0.09	0.51	1.35	0.47	0.49	0.67	21.94	23.09	54.97
	/	crude oil	Q601	1.52	0.62	0.49	0.29	0.36	0.89	0.31	0.22	0.48	25.17	24.76	50.07

[a]Note: R1 = pristane/phytane; R2 = gammacerane/C_{31} 22R hopane; R3 = $C_{35}S/C_{34}S$ homohopanes; R4 = C_{31} 22R/C_{30} hopanes; R5 = C_{19}/C_{23} tricyclic terpane; R6 = C_{26}/C_{25} tricyclic terpane; R7 = 18α-30-norneohopane/C_{29} hopane; R8 = 17α-diahopane (C_{30}*)/C_{30} hopane; R9 = C_{29} steranes ($\beta\beta/(\alpha\alpha + \beta\beta)$); R10 = %$C_{27}$ $\alpha\alpha\alpha$ R (e.g., %C_{27} $\alpha\alpha\alpha$ R = %$C_{27}\alpha\alpha\alpha$ R /(%$C_{27}\alpha\alpha\alpha$ R to %$C_{29}\alpha\alpha\alpha$ R); R11 = %C_{28} $\alpha\alpha\alpha$ R; R12 = %C_{29} $\alpha\alpha\alpha$ R.

h. All rock extracts and oils were further separated into saturate, aromatic, resin, and asphaltene fractions by column chromatography.

Gas chromatography−mass spectrometry (GC−MS) analysis was applied to the saturated fraction using SHIMADZU GC-2010Plus-MS OP2010 Ultra, equipped with an HP-5MS column (30 m long, 0.25 mm i.d., and 0.25 μm film thickness). The GC oven temperature was initially held at 50 °C for 2 min and increased to 120 °C at 20 °C/min, then to 250 °C at 4 °C/min, and finally to 310 °C at 3 °C/min and maintained for 30 min. The carrier gas was helium (400−700 kPa). The MS was performed in the positive electron ionization mode. The ion source temperature was 230 °C with an ionizing energy of 70 eV. The MS was operated in the selected ion monitoring mode (SIM) and a full scan in the 50−550 m/z mass range.

All powdered rock samples were used to perform X-ray diffraction (XRD) analysis, which was conducted on a Bruker D8 Advance diffractometer with a Ni filter and Cu Kα radiation. The instrument conditions were set as follows: operating voltage, 40 kV; operating current, 30 mA; scanning range, 2θ = 3−85°; silt, 1 mm; and scanning speed, 4/min.

3.3. Statistical Analysis. The correlation coefficient between the rearranged hopanes and other saturated biomarker parameters was determined using SPSS 22.0. Multiple biomarker proxies were used in the statistical analysis, including Pr/Ph, Ga/C_{31}R, $C_{35}S/C_{34}S$ hopanes, C_{31}R/H, $C_{19}TT/C_{23}TT$, $C_{26}TT/C_{25}TT$, %C_{27} $\alpha\alpha\alpha$ R sterane, %C_{28} $\alpha\alpha\alpha$ R sterane, %C_{29} $\alpha\alpha\alpha$ R sterane, $C_{29}Ts/C_{29}$, C_{30}*/H, and C_{29} $\beta\beta/(\alpha\alpha + \beta\beta)$. For any further information on these selected parameters, please refer to the study by Peters et al.[13]

4. RESULTS AND DISCUSSION

4.1. Geochemical Features of Source Rocks. As shown in Table 1, there is a wide variation in the Rock-Eval data of eight rocks from the Ordos Basin, North China Block, and Sichuan Basin. The total organic carbon (TOC) content of the studied rocks ranges from 13.08 to 16.07 wt %, 0.86 to 5.32 wt %, and 1.32 to 4.22 wt %, respectively. The hydrocarbon genetic potentials ($S_1 + S_2$) of these source rocks fall in the ranges of 55.91−78.49 mg HC/g rock, 2.31−19.36 mg HC/g rock, and 0.43−1.93 mg HC/g rock, respectively. These data suggest that those rocks from the Ordos Basin and North China Block are good source rocks, whereas source rocks from the Sichuan Basin have relatively a low hydrocarbon generation potential.[42] Hydrogen index (HI) of sample dxhy indicates mixed Type II/III, while HI values of samples from Songliao and Sichuan basins indicate Type II and Type IV, respectively.[43]

4.2. Distribution of Rearranged Hopanes. Three series of rearranged hopanes were identified in studied rock and oil samples from the North China Block and Sichuan, Ordos, and Tarim basins, in accordance with the relative retention time,

https://dx.doi.org/10.1021/acsomega.0c04615
ACS Omega 2020, 5, 30160−30167

mass spectral feature, peak sequence, and identification standards from prior research.[3,12,16,23,31] Compounds of rearranged hopane series contain the 18α(H)-neohopane series (Ts and C_{29}Ts), the 17α(H)-diahopane series (C_{29} and C_{30} rearranged hopanes), and the early-eluting rearranged hopane series (C_{30} early-eluting rearranged hopane or 30E) (Figure 2). All of the samples show a strong dominance of 18α(H)-neohopane and 17α(H)-diahopane series. The early-eluting rearranged hopane series (30E) is detected only in a small number of samples from the Tarim Basin and North China Block. Thus, two biomarker parameters of rearranged hopanes, including C_{29}Ts/C_{29} hopane and C_{30}*/C_{30} hopane, were mainly discussed in this paper.

4.3. Relationship between Clay Minerals and Rearranged Hopanes. XRD results of bulk samples show that the rock samples are principally composed of quartz, feldspar, illite, chlorite, kaolinite, calcite, dolomite, high-Mg calcite, siderite, and pyrite (Table 2). Great differences in mineral composition exist among samples from different regions. For example, quartz is dominant in two rock samples from the Xiamaling Formation. In contrast, illite is predominant in other samples from the Ordos and Sichuan basins.

The total content of clay minerals in all the source rocks ranges from 18.9 to 90.3%, with a mean value of 52.7%. Clay minerals are mainly illite, chlorite, and kaolinite. The relative abundance of rearranged hopanes is unlikely linked to the content of clay minerals, as suggested by a little correlation between the C_{29}Ts/C_{29} hopane or C_{30}*/C_{30} hopane ratio and clay content (Figure 3a,b). This is against the conventional wisdom that the rearranged hopanes are likely catalyzed by clay minerals.[3,5,13] This phenomenon corroborates the findings of source rocks in the Songliao Basin and Yabulai Basin.[18,44] Contrary to the clay content, a strong positive relationship between the relative concentration of rearranged hopanes and quartz was observed (Figure 3c,d). This may mean the quartz content in source rocks plays an essential role in the generation of rearranged hopanes.

4.4. Relationship between Rearranged Hopanes and Other Biomarkers. Biomarker compounds in rock extracts and oils are controlled by the sources and depositional environments of organic matter in sediments, whereas thermal maturity reflects the degree of thermally driven reactions that sedimentary organic material was converted to petroleum.[13] Therefore, Pearson correlation analysis (PCA) of source-, depositional environment-, and maturity-related biomarker parameters was used to examine the relationship between these biomarkers and the relative abundance of rearranged hopanes. PCA is a multivariate statistical method that improves the interpretation of geochemical data and widely applied in many disciplines.[45−48]

Twelve biomarker parameters as variables were selected to perform the PCA through SPSS statistical software (Table 3). For convenience, only two biomarker ratios of rearranged hopanes with other geochemical parameters were selected (Table 4 and Figure 4). Results of the PCA show that the two series of rearranged hopanes are well correlated with each other (R^2 = 0.9), probably indicating that they were produced by the same source.[13,16] Also, correlation coefficients between the C_{29}Ts/C_{29} hopane and other biomarker parameters decreased as follows: C_{31}R/H (R^2 = 0.74) > C_{35}S/C_{34}S (R^2 = 0.66) > C_{29} $\beta\beta/(\alpha\alpha+\beta\beta)$ (R^2 = 0.60) > %C_{27} $\alpha\alpha\alpha$ R (R^2 = −0.59) > %C_{28} $\alpha\alpha\alpha$ R (R^2 = 0.48) > C_{19}TT/C_{23}TT (R^2 = 0.43). Similarly, correlation coefficients between C_{30}*/H and other biomarker parameters decreased as follows: C_{31}R/H (R^2 = 0.87) > C_{35}S/C_{34}S (R^2 = 0.73) > C_{29} $\beta\beta/(\alpha\alpha+\beta\beta)$ (R^2 = 0.63) > %C_{27} $\alpha\alpha\alpha$ R (R^2 = −0.50) > C_{26}TT/C_{25}TT (R^2 = 0.47) > %C_{28} $\alpha\alpha\alpha$ R (R^2 = 0.43) > C_{19}TT/C_{23}TT (R^2 = 0.31).

Table 4. Correlation Analysis of the Relative Abundance of Rearranged Hopanes with Other Biomarker Parameters of Crude Oils and Source Rocks from the Ordos, Sichuan, and Tarim Basins and the North China Block

	C_{29}Ts/C_{29}	C_{30}*/H
C_{29}Ts/C_{29}	1	0.90
C_{30}*/H	0.90	1
Pr/Ph	0.16	0.26
C_{35}S/C_{34}S	0.66	0.73
C_{19}TT/C_{23}TT	0.43	0.31
C_{26}TT/C_{25}TT	0.35	0.47
C_{31}R/H	0.74	0.87
Ga/C_{31}22R	−0.03	−0.07
%C_{27} $\alpha\alpha\alpha$ R	−0.59	−0.50
%C_{28} $\alpha\alpha\alpha$ R	0.48	0.43
%C_{29} $\alpha\alpha\alpha$ R	0.25	0.19
C_{29} $\beta\beta/(\alpha\alpha+\beta\beta)$	0.60	0.63

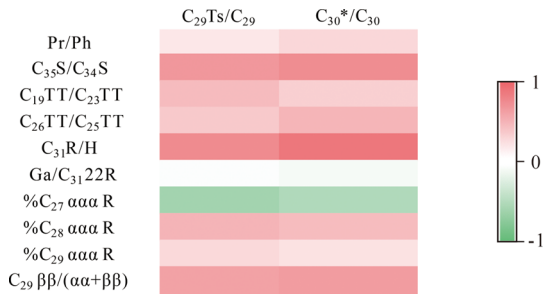

Figure 4. Heat plot of Pearson correlation coefficients of rearranged hopane ratios and other saturated biomarker proxies in rock and oil samples from the Ordos, Sichuan, and Tarim basins and the North China Block.

The PCA results suggest that those rock and oil samples with high rearranged hopane abundance are predominantly associated with the C_{31}R/H and C_{35}S/C_{34}S ratios followed by the C_{29} $\beta\beta/(\alpha\alpha+\beta\beta)$, %$C_{27}$ $\alpha\alpha\alpha$ R, and %C_{28} $\alpha\alpha\alpha$ R ratios and lastly the C_{26}TT/C_{25}TT and C_{19}TT/C_{23}TT ratios. C_{35}S/C_{34}S ratios are commonly used to reflect redox conditions,[49] whereas high values of the C_{31}R/C_{30} hopane and C_{26}TT/C_{25}TT ratios are closely related to the lacustrine source rocks.[13,50] These data may indicate that anoxic lacustrine conditions are favorable to generate a high concentration of rearranged hopanes. Moreover, the two rearranged hopane ratios are positively correlated with the C_{29} $\beta\beta/(\alpha\alpha+\beta\beta)$ sterane ratio, likely indicating that relatively high thermal maturity is also one of the major determinants to generate high abundance of rearranged hopanes.[3] Moreover, %C_{27} $\alpha\alpha\alpha$ R and C_{19}TT/C_{23}TT are negatively and positively correlated with the relative abundance of rearranged hopanes, respectively. There is a poor correlation between the rearranged hopanes and %C_{29} $\alpha\alpha\alpha$ R. The results show the rearranged hopanes to be related to lacustrine organic matter input.

In a word, the high concentration of rearranged hopanes in the studied rock and oil samples from the Songliao, Ordos, and Tarim basins and the North China Block may be principally related to the anoxic lacustrine environment and likely related

https://dx.doi.org/10.1021/acsomega.0c04615
ACS Omega 2020, 5, 30160−30167

to thermal maturity and terrigenous organic matter input, in terms of the correlation coefficient.

5. CONCLUSIONS

This paper proposed the controlling factors on relatively high abundance of rearranged hopanes in the studied rocks and oils from the Sichuan, Ordos, Tarim basins and the North China Block using multiple techniques. On the one hand, the rearranged hopane ratios are positively correlated with the content of quartz rather than that of clay. This is against the conventional wisdom that the rearranged hopanes are likely catalyzed by clay minerals. On the other hand, the correlation results of this systematical study of rocks and oils from representative basins in China show that the key controlling factor on the generation of abundant rearranged hopanes is the anoxic lacustrine environment. Lastly, PCA is a statistical method that can improve the interpretation of geochemical data through considering the effects of multiple parameters simultaneously. Thus, the method of this study may be applied into similar research studies in other sedimentary basins.

AUTHOR INFORMATION

Corresponding Author

Yao-Ping Wang − *College of Chemistry and Environmental Science, Guangdong Ocean University, Zhanjiang 524088, P.R. China; State Key Laboratory of Organic Geochemistry, Guangzhou Institute of Geochemistry, Chinese Academy of Sciences, Guangzhou 510640, P.R. China;* orcid.org/0000-0003-0994-6030; Email: wangyp@gdou.edu.cn

Authors

Xin Zhan − *CNOOC International Limited, Beijing 100027, P.R. China*

Yuan Gao − *College of Chemistry and Environmental Science, Guangdong Ocean University, Zhanjiang 524088, P.R. China*

Jia Xia − *College of Chemistry and Environmental Science, Guangdong Ocean University, Zhanjiang 524088, P.R. China*

Sibo Wang − *College of Chemistry and Environmental Science, Guangdong Ocean University, Zhanjiang 524088, P.R. China*

Yan-Rong Zou − *State Key Laboratory of Organic Geochemistry, Guangzhou Institute of Geochemistry, Chinese Academy of Sciences, Guangzhou 510640, P.R. China;* orcid.org/0000-0003-4071-6233

Complete contact information is available at: https://pubs.acs.org/10.1021/acsomega.0c04615

Notes

The authors declare no competing financial interest.

ACKNOWLEDGMENTS

This work was supported by the Doctoral Research Initiation Project of Guangdong Ocean University (Grant nos. R20030 and R17001), National Science Foundation of China (Grant no. 41602139), and the Special Financial Aid for Talents of Guangdong Ocean University (Grant no. 002026002004).

REFERENCES

(1) Peters, K. E.; Moldowan, J. M., *The Biomarker Guide: Interpreting Molecular Fossils in Petroleum and Ancient Sediments*. NJ (United States); Prentice Hall 1993, 1−363.

(2) Nytoft, H. P.; Lutnæs, B. F.; Johansen, J. E. 28-Nor-spergulanes, a novel series of rearranged hopanes. *Org. Geochem.* **2006**, *37*, 772−786.

(3) Moldowan, J. M.; Fago, F. J.; Carlson, R. M. K.; Young, D. C.; an Duvne, G.; Clardy, J.; Schoell, M.; Pillinger, C. T.; Watt, D. S. Rearranged hopanes in sediments and petroleum. *Geochim. Cosmochim. Ac.* **1991**, *55*, 3333−3353.

(4) Smith, M.; Bend, S. Geochemical analysis and familial association of Red River and Winnipeg reservoired oils of the Williston Basin, Canada. *Org. Geochem.* **2004**, *35*, 443−452.

(5) Farrimond, P.; TelnÆS, N. Three series of rearranged hopanes in Toarcian sediments (northern Italy). *Org. Geochem.* **1996**, *25*, 165−177.

(6) Killops, S. D.; Howell, V. J. Complex series of pentacyclic triterpanes in a lacustrine sourced oil from Korea Bay Basin. *Chem. Geol.* **1991**, *91*, 65−79.

(7) Philp, R. P.; Gilbert, T. D. Biomarker distributions in Australian oils predominantly derived from terrigenous source material. *Org. Geochem.* **1986**, *10*, 73−84.

(8) Telnaes, N.; Isaksen, G. H.; Farrimond, P. Unusual triterpane distributions in lacustrine oils. *Org. Geochem.* **1992**, *18*, 785−789.

(9) Cao, J.; Bian, L.; Hu, K.; Liu, Y.; Wang, L.; Yang, S.; Chen, Y.; Peng, X. Benthic macro red alga: A new possible bio-precursor of Jurassic mudstone source rocks in the northern Qaidam Basin, northwestern China. *Sci. China Ser. D* **2009**, *52*, 647−654.

(10) Zhang, S.; Zhang, B.; Bian, L.; Jin, Z.; Wang, D.; Chen, J. The Xiamaling oil shale generated through Rhodophyta over 800 Ma ago. *Sci. China Ser. D* **2007**, *50*, 527−535.

(11) Horstad, I.; Larter, S. R.; Dypvik, H.; Aagaard, P.; Bjørnvik, A. M.; Johansen, P. E.; Eriksen, S. Degradation and maturity controls on oil field petroleum column heterogeneity in the Gullfaks field, Norwegian North Sea. *Org. Geochem.* **1990**, *16*, 497−510.

(12) Li, M.; Lin, R.; Liao, Y.; Snowdon, L. R.; Wang, P.; Li, P. Org. Geochem. of oils and condensates in the Kekeya Field, Southwest Depression of the Tarim Basin (China). *Org. Geochem.* **1999**, *30*, 15−37.

(13) Peters, K. E.; Walters, C. C.; Moldowan, J. M., *The Biomarker Guide:Biomarkers and Isotopes in Petroleum and Earth History*. Cambridge: Cambridge University Press; 2005, 1155.

(14) Zhu, Y.; Zhong, R.; Cai, X.; Luo, Y. Composition and origin approach of rearranged hopanes in Jurassic oils of central Sichuan Basin. *Geochimica* **2007**, *36*, 253−260 (in Chinese with English abstract).

(15) Yang, W.; Liu, G.; Feng, Y. Geochemical significance of 17α(H)-diahopane and its application in oil-source correlation of Yanchang formation in Longdong area, Ordos basin, China. *Mar. Petrol. Geol.* **2016**, *71*, 238−249.

(16) Jiang, L.; George, S. C.; Zhang, M. The occurrence and distribution of rearranged hopanes in crude oils from the Lishu Depression, Songliao Basin, China. *Org. Geochem.* **2018**, *115*, 205−219.

(17) Kong, T.; Zhang, M. Effects of depositional environment on rearranged hopanes in lacustrine and coal measure rocks. *J. Petrol. Sci. Eng.* **2018**, *169*, 785−795.

(18) Jin, X.; Zhang, Z.; Wu, J.; Zhang, C.; He, Y.; Cao, L.; Zheng, R.; Meng, W.; Xia, H. Origin and geochemical implication of relatively high abundance of 17α (H)-diahopane in Yabulai basin, northwest China. *Mar. Petrol. Geol.* **2019**, *99*, 429−442.

(19) Zhang, M.; Li, H.; Wang, X. Geochemical characteristics and grouping of the crude oils in the Lishu fault depression, Songliao basin, NE China. *J. Petrol. Sci. Eng.* **2013**, *110*, 32−39.

(20) Liu, G.; Yang, W.; Feng, Y.; Ma, H.; Du, Y. Geochemical characteristics and genetic types of crude oils from Yanchang Formation in Longdong Area. *Ordos Basin. Earth Sci. Front.* **2013**, *20*, 108−115 (in Chinese with English abstract).

(21) Zhang, W.; Yang, H.; Hou, L.; Liu, F. Distribution and geological significance of 17α(H)-diahopanes from different hydrocarbon source rocks of Yanchang Formation in Ordos Basin. *Sci. China Ser. D* **2009**, *52*, 965−974.

(22) Zhu, Y.; Hao, F.; Zou, H.; Cai, X.; Luo, Y. Jurassic oils in the central Sichuan basin, southwest China: Unusual biomarker distribution and possible origin. *Org. Geochem.* **2007**, *38*, 1884−1896.
(23) Wang, X.; Zhao, W.; Zhang, S.; Wang, H.; Su, J.; Canfield, D. E.; Hammarlund, E. U. The aerobic diagenesis of Mesoproterozoic organic matter. *Sci. Rep.* **2018**, *8*, 13324.
(24) Dai, J.; Gong, D.; Ni, Y.; Huang, S.; Wu, W. Stable carbon isotopes of coal-derived gases sourced from the Mesozoic coal measures in China. *Org. Geochem.* **2014**, *74*, 123−142.
(25) Yang, J. J., *Tectonic Evolution and Oil-Gas Reservoirs Distribution in Ordos Basin*. Petroleum Industry Press: Beijing (in Chinese), 2002, 1−228.
(26) Duan, Y.; Wu, Y. Distribution and formation of Mesozoic low permeability underpressured oil reservoirs in the Ordos Basin, China. *J. Petrol. Sci. Eng.* **2020**, *187*, 106755.
(27) Duan, Y.; Wang, C. Y.; Zheng, C. Y.; Wu, B. X.; Zheng, G. D. Geochemical study of crude oils from the Xifeng oilfield of the Ordos basin, China. *J. Asian Earth Sci.* **2008**, *31*, 341−356.
(28) Liu, Y.; Chen, D.; Qiu, N.; Fu, J.; Jia, J. Geochemistry and origin of continental natural gas in the western Sichuan basin, China. *J. Nat. Gas Sci. Eng.* **2018**, *49*, 123−131.
(29) Zheng, T.; Ma, X.; Pang, X.; Wang, W.; Zheng, D.; Huang, Y.; Wang, X.; Wang, K. Org. Geochem. of the Upper Triassic T3x5 source rocks and the hydrocarbon generation and expulsion characteristics in Sichuan Basin, central China. *J. Petrol. Sci. Eng.* **2019**, *173*, 1340−1354.
(30) Li, Y.; Chen, S.; Wang, Y.; Qiu, W.; Su, K.; He, Q.; Xiao, Z. The origin and source of the Devonian natural gas in the Northwestern Sichuan Basin, SW China. *J. Petrol. Sci. Eng.* **2019**, *181*, 106259.
(31) Jin, X.; Pan, C.; Yu, S.; Li, E.; Wang, J.; Fu, X.; Qin, J.; Xie, Z.; Zheng, P.; Wang, L.; Chen, J.; Tan, Y. Org. Geochem. of marine source rocks and pyrobitumen-containing reservoir rocks of the Sichuan Basin and neighbouring areas, SW China. *Mar. Petrol Geol.* **2014**, *56*, 147−165.
(32) Zhang, S.; Li, Z.-X.; Evans, D. A. D.; Wu, H.; Li, H.; Dong, J. Pre-Rodinia supercontinent Nuna shaping up: A global synthesis with new paleomagnetic results from North China. *Earth Planet. Sci. Lett.* **2012**, *353-354*, 145−155.
(33) Gao, L.; Zhang, C.; Shi, X.; Song, B.; Wang, Z.; Liu, Y. Mesoproterozoic age for Xiamaling Formation in North China Plate indicated by zircon SHRIMP dating. *Chin. Sci. Bull.* **2008**, *53*, 2665−2671.
(34) Su, W.; Zhang, S.; Huff, W. D.; Li, H.; Ettensohn, F. R.; Chen, X.; Yang, H.; Han, Y.; Song, B.; Santosh, M. SHRIMP U−Pb ages of K-bentonite beds in the Xiamaling Formation: Implications for revised subdivision of the Meso- to Neoproterozoic history of the North China Craton. *Gondwana Res.* **2008**, *14*, 543−553.
(35) Zhang, S.; Wang, X.; Wang, H.; Hammarlund, E. U.; Su, J.; Wang, Y.; Canfield, D. E. The oxic degradation of sedimentary organic matter 1400 Ma constrains atmospheric oxygen levels. *Biogeosciences* **2017**, *14*, 2133−2149.
(36) Zhang, S.; Wang, X.; Hammarlund, E.; Mafalda, H. Orbital forcing of climate 1.4 billion years ago. *P. Natl. Acad. Sci. USA* **2015**, *112*, E1406−E1413.
(37) Chen, Z.; Wang, T. G.; Li, M.; Yang, F.; Cheng, B. Biomarker geochemistry of crude oils and Lower Paleozoic source rocks in the Tarim Basin, western China: An oil-source rock correlation study. *Mar. Petrol. Geol.* **2018**, *96*, 94−112.
(38) Zhang, S. C.; Hanson, A. D.; Moldowan, J. M.; Graham, S. A.; Liang, D. G.; Chang, E.; Fago, F. Paleozoic oil−source rock correlations in the Tarim basin, NW China. *Org. Geochem.* **2016**, *94*, 32−46.
(39) Chang, X. C.; Wang, T.-G.; Li, Q. M.; Ou, G. X. Charging of Ordovician reservoirs in the Halahatang depression (Tarim Basin, NW China) determined by oil geochemistry. *J. Petrol. Geol.* **2013**, *36*, 383−398.
(40) He, D.; Li, D.; He, J.; Wu, X. Comparison in petroleum geology between Kuqa depression and Southwest depression in Tarim Basin and its exploration significance. *Ac. Petrol. Sin.* **2013**, *34*, 201−218. (in Chinese with English abstract)
(41) Wu, X.; Tao, X.; Hu, G. Geochemical characteristics and source of natural gases from Southwest Depression of the Tarim Basin, NW China. *Org. Geochem.* **2014**, *74*, 106−115.
(42) Peters, K. E. Guidelines for evaluating petroleum source rock using programmed prolysis. *AAPG Bull.* **1986**, *70*, 318−329.
(43) Peters, K. E.; Cassa, M. R., Applied source rock geochemistry. *In: the petroleum system: from source to trap*, Magoon, L.B.; Dow, W.G. (Eds.), 60. *AAPG Mem.* 1994, 93−120.
(44) Jiang, L. Study on rearranged hopanes in hydrocarbon source rocks and crude oils in the Songliao Basin, NE China. Master degree, Yangtze University (in Chinese) , 2016.
(45) Sato, A.; Zhang, T.; Yonekura, L.; Tamura, H. Antiallergic activities of eleven onions (Allium cepa) were attributed to quercetin 4′-glucoside using QuEChERS method and Pearson's correlation coefficient. *J. Funct. Foods* **2015**, *14*, 581−589.
(46) Mu, Y.; Liu, X.; Wang, L. A Pearson's correlation coefficient based decision tree and its parallel implementation. *Inform. Sciences* **2018**, *435*, 40−58.
(47) Kalpana, M. S.; Madhavi, T.; Mani, D.; Lakshmi, M.; Pundaree, N.; Sujai, M.; Kavitha, S.; Devekar, A. P.; Patil, D. J.; Dayal, A. M.; Haragopal, V. Integrated surface geochemical studies for hydrocarbon prospects in Deccan Syneclise, India. *J. Petrol. Sci. Eng.* **2016**, *147*, 801−815.
(48) Puth, M.-T.; Neuhäuser, M.; Ruxton, G. D. Effective use of Pearson's product−moment correlation coefficient. *Anim. Behav.* **2014**, *93*, 183−189.
(49) Peters, K. E.; Moldowan, J. M. Effects of source, thermal maturity, and biodegradation on the distibution and isomerization of homohopanes in petroleum. *Org. Geochem.* **1991**, *17*, 47−61.
(50) Schiefelbein, C. F.; Zumberge, J. E.; Cameron, N.; Brown, S. Petroleum systems in the South Atlantic margins. *Geol. Soc., Spl. Pub.: London* **1999**, *153*, 169−179.

https://dx.doi.org/10.1021/acsomega.0c04615
ACS Omega 2020, 5, 30160−30167